INTERNATIONAL
Agrophysics
www.international-agrophysics.org

Int. Agrophys., 2025, 39, 475-488
doi: 10.31545/intagr/204156

Optimization of parboiling conditions and nitrogen fertilization for brown rice quality: textural properties, phytic acid content, and mineral composition

Azin Nasrollah zade, Mandana Tayefe*

Department of Food Science and Technology, La.C., Islamic Azad University, Lahijan, Iran, Postal Code: 4416939515
Postal box: 1616, Iran

Received August 12, 2024; accepted January 21, 2025

Abstract. A 5-level, 3-factor central composite rotatable design in response surface methodology (RSM) was used to optimize the effects of parboiling operating parameters (soaking temperature (SoTe, 39.8-90.2°C) and steaming time (StTi, 8.3-16.7 min)) and nitrogen fertilizer (NF, 46.4-113.6 kg ha^{-1}) levels on physicomechanical (hardness and ΔE color values) and nutritional properties (zinc (Zn), iron (Fe), calcium (Ca), phytic acid (PA), and PA/Zn) of protein-rich brown rice. Sensory evaluation showed that consumers preferred rice grains with a relatively soft texture and medium hardness. The experimental data fit well to second-order polynomial models ($R^2 \geq 0.976$) using multiple regression analysis. The optimum conditions for maximizing mineral content (Zn: 385.0 ppm, Fe: 78.0 ppm, Ca: 33.0 ppm), minimizing PA content (130.91 mg 100 g^{-1}), PA/Zn ratio (0.34), achieving a low ΔE value (4.71), and obtaining the desired hardness (17.0 N) were 59.29°C SoTe, 11.18 min StTi, and 90.89 kg ha^{-1} NF.

Keywords: rice (*Oryza sativa* L.), parboiling, N fertilizer, antinutritional factor, minerals, process optimization

1. INTRODUCTION

Rice is the second most commonly produced cereal in the world as it is consumed by over half of the global population (Gharibzahedi, 2018). According to USDA data, the total global rice production in 2022 was 776 million tons (Glauber and Mamun, 2025). Rice is a rich source of protein, fiber, carbohydrates, vitamins (*e.g.*, thiamin and niacin), and minerals (*e.g.*, iron (Fe), zinc (Zn), and phosphorus (P)) (Yu *et al*., 2021). This staple food also contains antioxidant compounds, including phenolic acids, γ-oryzanol, anthocyanin, and proanthocyanidins (Kumar *et al*., 2017). Rice consists of 72% endosperm, 20% hulls, and 8% bran. However, rice processing, including the removal of hulls, the milling of shelled rice to eliminate the bran layer, and an extra whitening step, can exacerbate the loss of these nutrients with a further reduction in their content and bioavailability rate (Park *et al*., 2019). Also, rice has the antinutritional compound phytic acid (PA), which is indigestible to humans or nonruminants owing to a lack of phytase. PA can inhibit the absorption and bioavailability of minerals through the formation of strong molecular complexes with Fe and Zn, decreasing the nutritional value of rice-based foods (Xia *et al*., 2019). Although brown rice contains higher amounts of protein, vitamins, and minerals compared to white milled rice, the higher levels of PA can reduce the solubility, functionality, absorption, and bioaccessibility of essential minerals such as Fe and Zn. This issue is of considerable importance because 2 billion and 3-4 billion people worldwide suffer from Fe and Zn deficiency, respectively (Kumar *et al*., 2017).

There are various technological processes to reduce the PA content in the food industry, such as soaking, heating (*e.g.*, baking, autoclaving, frying), malting, and fermentation. However, none of these processing techniques can eliminate PA from rice grains (Özkaya *et al*., 2017; Tayefe *et al*., 2020). Currently, the use of enzymatic treatments and non-thermal processes, such as high-pressure, pulsed electric field, cold plasma, and ultrasound, has efficiently improved the quality and health attributes of wholegrain brown rice (Gharibzahedi *et al*., 2018; Xia *et al*., 2019).

© 2025 Institute of Agrophysics, Polish Academy of Sciences

*Corresponding author e-mail: azinnasr@yahoo.com

Parboiling is widely recognized as the most important step in the pre-processing of rice grain in many rice-producing countries in Asia. This process not only successfully extends the storage stability of rice grains but also minimizes nutritional losses while increasing mineral bioavailability and reducing PA content (Paiva *et al*., 2016; Patindol *et al*., 2017). On the other hand, starch gelatinization and retrogradation irreversibly change the microstructure of the biopolymer during the soaking and steaming stages of this hydrothermal process, resulting in different digestibility and textural properties of parboiled rice compared to polished rice (Tian *et al*., 2018). Our recent study has shown that the integrated use of the parboiling process and nitrogen fertilization (NF) can significantly improve the chemomechanical, rheological, and pasting characteristics of brown rice grains (BRGs). However, excessive or insufficient NF application reduced the production yield and the technological and nutritional quality of rice grains (Nasrollah Zadeh *et al*., 2020). Therefore, there is a necessity to optimize NF levels and parboiling conditions, including soaking temperature (SoTe) and steaming time (StTi), to achieve the best quality and nutritional values of parboiled BRGs.

Response surface methodology (RSM) is a well-known statistically based mathematical optimization approach that can simultaneously construct adequate models for independent (input) and response (output) variables (Gharibzahedi *et al*., 2015a). This simple mathematical tool decreases the cost of product formulations and processes by reducing the number of required tests (Rostami and Gharibzahedi, 2017). RSM provides solutions to multi-objective functions to produce an optimum response by estimating their composite desirability (Gharibzahedi *et al*., 2012).

To the best of our knowledge, this simple and efficient modeling approach has not yet been used to predict the optimal parboiling conditions and NF levels for yielding the best technological quality and nutritional value of BRGs. Thus, the present study was aimed to optimize the combined operational conditions for producing nutritious parboiled BRGs with the goal of achieving greater consumer preference and more market share. We hypothesize that optimized parboiling conditions combined with precise nitrogen fertilization will: (i) significantly reduce PA content through thermal degradation and enzymatic activation during processing, and (ii) enhance mineral retention by modifying rice kernel microstructure and regulating nutrient assimilation pathways. These effects are anticipated to result from the synergistic interaction between parboiling-induced physicochemical transformations and nitrogen-mediated metabolic regulation in the rice plant.

2. MATERIALS AND METHODS

2.1. Rice cultivation conditions and fertilization practices

One of the most commonly cultivated rice varieties in Iran, namely Hashemi, was cultivated at the farm of the National Institute of Rice Research (NIRR, Rasht, Gilan province, Iran; 37°20′N, 49°40′E, altitude 5 m) in May 2019 using a conventional transplanting method and harvested during August-September 2019. Hashemi rice, a traditional and widely cultivated variety in northern Iran (particularly in Gilan and Mazandaran provinces), was selected for this study due to its high consumer preference, distinctive aroma, superior cooking quality, and its recognized status in agricultural improvement programs aimed at enhancing yield and grain purity.

Field experiments were conducted using uniformly sized plots (5 × 3 m) with controlled growing conditions. Manual weed control was implemented at two critical growth stages to minimize competition. Water management maintained a constant 5 cm standing water level from transplanting to flowering to ensure optimal growing conditions. No chemical pesticides were applied during the experiment. Weed management was conducted manually at two critical growth stages to minimize competition. Before fertilization, triplicate soil samples were collected from randomized locations within the experimental field and analyzed at the NIRR laboratories. The average soil properties at the NIRR farm (Rasht, Gilan province, Iran) included 46% clay, 42% silt, and 12% sand, with a saturation percentage of 82.1%, electrical conductivity (EC) of 1.34 dS m^{-1}, pH of 6.74, and 2.08% organic carbon. According to recommendations of the Soil and Water Research Institute (SWRI, Tehran, Iran), we applied 50 kg ha^{-1} of phosphorus pentoxide (P_2O_5) and 25 kg ha^{-1} of potassium oxide (K_2O) for the cultivated rice. To increase rice grain yield, the soil of the rice fields was also fertilized with five NF levels from 46.4 to 113.6 kg ha^{-1} based on the RSM design (Table 1). Preliminary field studies showed that NF levels outside this range significantly reduced rice grain yield.

2.2. Chemicals

All chemicals used, such as ethanol (EtOH), hydrochloric acid (HCl), nitric acid (HNO_3), 5-sulfosalicylic acid dihydrate, iron(III) chloride ($FeCl_3$), glutaraldehyde, osmium tetroxide, and phosphate buffer, were purchased from Sigma-Aldrich Chemical Co. (Oakville, ON, Canada).

2.3. Parboiling processing of brown rice

Parboiling of paddy rice followed various soaking and steaming regimes (Table 1). The soaking setup included a stainless steel cylindrical container, an electric heater, a basket for water-soaking, and a temperature control system (NSS-450, Nojan Co., Tehran, Iran). For each treatment, ~200 g of BRGs were soaked in deionized water (1 L) in a water bath at 39.8-90.2°C (SoTe) for 6 h (Table 1). Soaked BRGs were removed from the water to allow water penetration into the grain core and then placed in a plastic bag at 25±2°C for 4 h. A total of 150 g of soaked BRGs were placed in a parboiling vessel above a boiler containing 8 L

Table 1. RSM-CCRD matrix based on the independent variables and experimental results of response variables

No.	Independent variables[a]				Response variables					
	SoTe (°C)	StTi (min)	NF (kg ha^{-1})	Hardness (N)	ΔE	PA (mg 100 g)	Zn	Fe	Ca	PA/Zn
							(ppm)			
1	50	10	60	15.3±0.1	2.9±0.2	266±7	345.6±1.7	78.1±1.6	36.7±0.1	0.769±0.027
2	80	10	60	16.0±0.2	6.7±0.0	200±6	364.1±6.1	62.3±0.4	25.6±0.2	0.549±0.035
3	50	15	60	15.7±0.1	3.1±0.0	246±4	320.6±5.3	60.8±0.7	28.6±0.4	0.767±0.026
4	80	15	60	16.2±0.1	7.5±0.2	174±4	375.0±0.8	52.1±2.4	21.3±0.4	0.464±0.015
5	50	10	100	17.5±0.1	8.4±0.3	154±2	392.3±3.6	84.2±0.2	33.4±0.5	0.392±0.001
6	80	10	100	18.9±0.0	10.5±0.0	159±1	401.5±0.8	63.4±1.9	25.8±0.5	0.396±0.013
7	50	15	100	18.0±0.0	8.6±0.0	132±5	340.9±1.6	63.8±2.2	24.7±0.7	0.387±0.022
8	80	15	100	19.4±0.1	11.4±0.2	128±6	368.2±2.7	56.0±0.9	20.8±0.6	0.347±0.014
9	39.8	12.5	80	15.8±0.1	3.8±0.3	258±2	351.2±3.2	80.0±1.6	34.7±0.6	0.734±0.011
10	90.2	12.5	80	17.4±0.2	10.3±0.2	201±1	397.1±3.1	58.5±2.1	22.1±0.4	0.506±0.007
11	65	8.3	80	16.4±0.2	8.3±0.2	198±5	377.3±4.2	81.0±1.2	35.4±0.9	0.524±0.022
12	65	16.7	80	17.1±0.1	10.0±0.2	169±2	332.3±2.1	60.0±2.5	25.5±0.2	0.508±0.003
13	65	12.5	46.4	14.9±0.2	1.1±0.0	165±12	364.1±6.1	63.0±1.8	27.5±1.1	0.453±0.055
14	65	12.5	113.6	19.4±0.1	9.1±0.0	71±10	395.0±0.2	69.0±1.9	25.8±0.0	0.179±0.036
15	65	12.5	80	16.8±0.1	3.5±0.3	138±5	367.2±8.4	70.9±0.3	31.8±0.5	0.375±0.023
16	65	12.5	80	16.6±0.0	2.9±0.3	135±2	373.3±2.3	70.6±0.6	32.2±0.3	0.361±0.009
17	65	12.5	80	16.8±0.1	3.3±0.1	139±6	379.5±3.9	71.5±0.2	32.1±0.1	0.366±0.014
18	65	12.5	80	16.4±0.3	3.1±0.1	128±4	375.3±0.3	73.3±2.0	31.9±0.0	0.341±0.010
19	65	12.5	80	16.9±0.3	2.9±0.3	133±1	380.1±4.5	72.5±1.2	31.7±0.6	0.350±0.001
20	65	12.5	80	16.7±0.0	3.4±0.2	124±8	377.31±1.5	68.2±2.4	30.5±1.2	0.320±0.031

[a] SoTe – soaking temperature, StTi – Steaming time, NF – nitrogen fertilization. Data are represented as mean±SD (n = 3).

of boiling water and steamed at low pressure (78.45 kPa) at 119°C for 8.3-16.7 min (StTi, Table 1) (Nasrollah Zadeh *et al*., 2020). SoTe and StTi values were selected based on preliminary quality data. Steamed samples were spread on trays and dried in a hot-air oven (ATRA, ACE400L, Qazvin, Iran) at 52±2°C for 8 h to reduce moisture content to 13% w.b. Tray positions were rotated several times to ensure uniform drying (Chavan *et al*., 2018). Parboiled samples were de-hulled and milled using a rice huller (ST50 model, Yanmar Co., Osaka, Japan) to produce BRGs.

2.4. Analysis of amylose and protein contents

Nitrogen content was measured using the Kjeldahl method, and total protein content (PC) was calculated by multiplying the nitrogen value by a conversion factor of 5.95. Amylose content (AC) was determined using a simplified method based on starch-iodine colorimetry (Nasrollah Zadeh *et al*., 2020).

2.5. Sensory evaluation

A sensory evaluation test was conducted to determine whether maximum, minimum, or median hardness was acceptable to consumers. This quality analysis involved 30 panelists, including graduate students and staff members of Islamic Azad University (Lahijan, Iran), familiar with the organoleptic qualities of parboiled BRGs. They included 16 women and 14 men aged 25-42 years. Samples were presented in a randomized order. The panelists evaluated the texture of each sample twice in well-lit conditions using a 9-point hedonic scale (1 = "really disliked" to 9 = "really liked"). Simultaneously, the samples were transferred to a texture analysis laboratory for hardness measurement.

2.6. Instrumental texture analysis

A texture analyzer machine (TA.XT Plus, Stable Micro Systems, Ltd, Surrey, England) equipped with a 500 N load cell and integrator was used to measure the hardness value of parboiled BRGs. The force measurement accuracy during sample deformation was 0.001 N. For this test, each grain placed between two 12-mm flat probes and compressed until rupture occurred in the force-deformation curve (Taghinezhad *et al*., 2016). The equivalent force at grain breakage in the force-deformation curve was considered to be the hardness value under a loading rate of 1 mm min^{-1} (Taheri-Garavand *et al.*, 2012). All samples were examined in triplicate.

2.7. Color measurement

A HunterLab colorimeter (model DP-900, Reston, VA, USA) was used to measure color attributes in the CIE L^*, a^*, b^* color space under the illuminant condition D65 (medium daylight) and a 10° (field of view) standard

observer. L^* is a measure of the lightness from black (0) to white (100). In the CIE L^*, a^*, b^* system, a^* and b^* are the chromaticity coordinates. Positive and negative a^* values respectively indicate the red and green directions, and positive and negative b^* values respectively are the yellow and blue directions. The total color difference (ΔE) was also calculated using the following equation (Eq. 1) (Tayefe *et al*., 2020):

$$\Delta E = \sqrt{(L - L^*)^2 + (a - a^*)^2 + (b - b^*)^2}, \quad (1)$$

where: L, a, and b values are color attributes for the untreated sample.

2.8. Determination of PA content

The content of PA was assessed according to the method described by Kaur *et al.* (2017) with minor modifications. In brief, PA was extracted from powdered BRGs (0.5 g) with 3.5% HCl (10.0 mL) under mild stirring for 90 min and centrifuged at 10 000 ×g, 5°C for 15 min. The obtained supernatant (1.0 mL) was diluted with 3.5% HCl (2 mL), and subsequently, 1.0 mL of the pink-colored Wade reagent (WR, 0.03 g ferric chloride dissolved in 100 mL of 0.3% 5-sulphosalicylic acid solution) was added and centrifuged. The solution absorbance was read using a UV-vis spectrophotometer (UVmini-1240, Shimadzu, Tokyo, Japan) at 500 nm. A decrease in the intensity of the pink color of WR occurs in the presence of phytate because iron can be sequestered and unavailable to react with 5-sulphosalicylic acid.

2.9. Assessment of essential mineral elements

The modified method proposed by Shao *et al.* (2018) was used to determine the content of Zn, Fe, and Ca of parboiled BRGs. In brief, 0.5 g of BRGs was hydrolyzed with 5 mL of ultrapure HNO_3 in a microwave digestion system with the power of 600 W (Sineo, Shanghai, China). The digestion procedure was as follows: temperature increase from 25 to 120°C, holding at 120°C for 7 min, raising to 180°C from 120°C over 15 min, and holding at 180°C for 25 min. The resulting solution, after cooling to 25°C was transferred to a volumetric flask and diluted with deionized water to 50 mL. Inductively coupled plasma-optical emission spectrometry (ICP-OES; Spectro Arcos, Germany) was used to measure Zn, Fe, and Ca at wavelengths of 213.9, 259.9, and 393.366 nm, respectively. The data were expressed as mg/kg of dry rice flour. All the experiments were performed in triplicate.

2.10. Statistical design and response surface optimization

A 5-level 3-factor response surface methodology-central composite rotatable design (RSM-CCRD) was used to evaluate the effects of SoTe (X_1, 39.8-90.2°C), StTi (X_2, 8.3-16.7 min), and NF level (X_3, 46.4-113.6 kg ha^{-1}) on the hardness value (Y_1), ΔE value (Y_2), and the content of PA (Y_3), Zn (Y_4), Fe (Y_5), Ca (Y_6), and PA/Zn (Y_7). The present study was mainly aimed to find out an optimum level of independent variables leading to (i) maximum mineral content of Zn, Fe, and Ca, (ii) minimum PA, PA/Zn, and ΔE levels, and (iii) a suitable hardness value depending on the sensory evaluation results. The experimental plan contained 20 trials, and the independent variables were investigated at three different levels, namely low (-1), medium (0), and high (+1), whose values were illustrated in Table 1. The experiments were randomized to minimize the effects of unexplained variability in the observed responses due to extraneous factors. The Design-Expert (trial version 8.1.6, Stat-Ease Inc., Minneapolis, USA) software was used to analyze the RSM-CCRD results. The linear, quadratic, and interaction effects of the studied three variables on the response variables were assessed. Analysis of variance (ANOVA) was performed to evaluate the statistical significance of the model. The response function (Y) related to the coded variables was fitted with second-order polynomial models using Eq. (2):

$$Y = b_0 + b_1X_1 + b_2X_2 + b_3X_3 + b_{11}X_1^2 + b_{22}X_2^2 + b_{33}X_3^2 + b_{12}X_1X_2 + b_{13}X_1X_3 + b_{23}X_2X_3 + \varepsilon. \quad (2)$$

The coefficients of the polynomial were denoted by b_0 (constant term), b_1, b_2, and b_3 (linear effects), b_{11}, b_{22}, and b_{33} (quadratic effects), and b_{12}, b_{13}, and b_{23} (interaction effects).

The terms found statistically non-significant ($p>0.05$) were removed from the initial models, and the experimental data were refitted to generate the final reduced models. The correlation between the response and independent variables is clearly depicted in the response surface and contour plots. The adequacy of regression models was evaluated by determination of R^2, adjusted R^2 (R^2_{adj}), coefficient of variation (CV, %), and adequate precision (AP) as previously recommended by Gharibzahedi *et al.* (2015). Five additional confirmation experiments were ultimately carried out to verify the accuracy of statistical experimental design. Also, the ANOVA procedure followed by Duncan's test was conducted for texture-based sensory properties using SPSS 20.0 (SPSS Inc., Chicago, IL, USA) software. Any significant difference between the means at a confidence level of 0.05 was examined. Furthermore, some data were a mean of three experimental replications and subjected to ANOVA using SPSS V.21 software (IBM Corp., Armonk, NY, USA). Significant differences were assessed by Duncan's test ($p<0.05$). Pearson's coefficient was used in the correlation analysis between hardness values and TA or TP levels.

3. RESULTS AND DISCUSSION

3.1. Sensory attributes

Hardness is one of the most significant quality characteristics of cooked rice grains. The evaluation results of

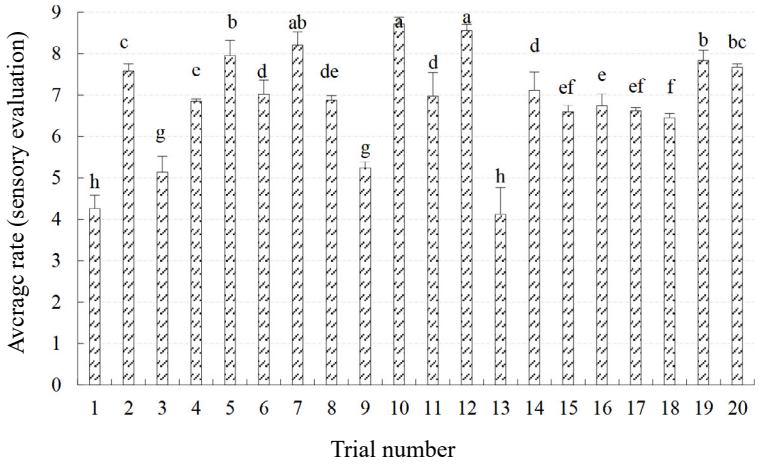

Fig. 1. Consumer linking of the parboiled BRGs produced at different experimental treatments. Avcragc ratings of thc samplcs with various lettcrs had a significant statistical diffcrcncc ($p<0.05$). The data are average of two replications (see Table 1 for hardness value of each experimental trial).

sensory attributes indicated that most panelists significantly preferred parboiled BRGs with a relatively soft texture (Fig. 1). These samples with a mean hardness value of 17.0-17.3 N were found to have the best hardness with maintaining favorable taste and flavor/odor. Accordingly, a targeted point of 17.15 N was considered to be the best hardness value to achieve the best overall organoleptic acceptability for the parboiled samples during the optimization studies.

3.2. Significance analysis and model fitting adequacy

Table 1 shows the design matrix of the independent variables in actual units along with the experimental values of response variables. By applying multiple regression analysis methods, the second-order polynomial models were adequate to predict the response (Table 2). ANOVA indicated that the fitted quadratic models were highly significant ($p<0.0001$). The lack-of-fit (LoF) test measures model failure to represent data in the experimental domain at points that are not included in the regression. Non-significant LoF is desirable to indicate model adequacy (Rostami and Gharibzahedi, 2017). The non-significant LoF values (0.0601-0.3289) of the fitted second-order polynomial models were statistically non-significant for the studied characteristics. The R^2 values ranged from 0.9762 to 0.9960, implying that only 2.38% of the variation in the worst possible case could not be explained by the fitted model (Table 3). The R^2_{adj} values (0.9251-0.9925) showed that the models were meaningful, and that the experimental values were in good agreement with the predicted ones.

Table 2. Reduced fitted second-order polynomial models and statistical parameters for response variables

Equation[a]	LoF[b]	Regression[b]	R^2	R^2_{adj}	CV[c]	AP
Hardness (N, Y_1)						
$16.69+0.49X_1+0.20X_2+1.33X_3+0.20X_1X_3+0.22X_3^2$	0.2972	< 0.0001	0.9856	0.9727	1.22	30.71
ΔE (-, Y_2)						
$3.18+1.76X_1+0.36X_2+2.35X_3-0.41X_1X_3+1.38X_1^2+2.12X_2^2+0.69X_3^2$	0.3289	< 0.0001	0.9960	0.9925	4.76	51.33
PA (mg 100 g^{-1}, Y_3)						
$132.25-17.05X_1-10.82X_2-34.49X_3+17.38X_1X_3+34.92X_1^2+18.65X_2^2$	0.2181	< 0.0001	0.9848	0.9712	5.11	33.12
Zn (ppm, Y_4)						
$375.6+13.66X_1-12.78X_2+10.95X_3+6.75X_1X_2-4.55X_1X_3-8.82X_2X_3-8.47X_2^2$	0.3253	< 0.0001	0.9678	0.9388	1.45	19.72
Fe (ppm, Y_5)						
$71.27-6.54X_1-6.64X_2+1.77X_3+2.51X_1X_2-2.53X_3^2$	0.1530	< 0.0001	0.9606	0.9251	3.52	17.65
Ca (ppm, Y_6)						
$31.74-3.74X_1-3.13X_2-0.76X_3+0.94X_1X_2+0.86X_1X_3-1.42X_1^2-0.69X_2^2-2.04X_3^2$	0.1339	< 0.0001	0.9830	0.9678	2.98	25.34
PA/Zn (-, Y_7)						
$0.35-0.069X_1-0.012X_2-0.11X_3+0.061X_1X_3+0.098X_1^2+0.061X_2^2$	0.0601	< 0.0001	0.9762	0.9548	7.27	25.82

[a]X_1, X_2, and X_3 are SoTe – soaking temperature (°C), StTi – steaming time (min), and NF – nitrogen fertilization (kg ha^{-1}), respectively.
[b]LoF – lack of fit (represented as p-value), [c]expressed as percentage (%).

Table 3. ANOVA of fitted quadratic models for the response variables

Source[a]	DF	Hardness (N)[b]				ΔE (-)				PA (mg 100 g^{-1})			
		SS	MS	F-value	P-value[c]	SS	MS	F-value	P-value	SS	MS	F-value	P-value
X_1	1	3.28	3.28	77.21	<0.0001	42.29	42.29	511.39	<0.0001	3970.5	3970.5	55.45	<0.0001
X_2	1	0.56	0.56	13.30	0.0045	1.8	1.8	21.78	0.0009	1598.9	1598.9	22.33	0.0008
X_3	1	24.17	24.17	569.29	<0.0001	75.71	75.71	915.52	<0.0001	16250	16250	226.95	<0.0001
X_{11}	1	0.0086	0.0086	0.20	ns	27.35	27.35	330.74	<0.0001	17569	17569	245.37	<0.0001
X_{22}	1	0.087	0.087	2.04	ns	64.77	64.77	783.32	<0.0001	5013	5013	70.03	<0.0001
X_{33}	1	0.69	0.69	16.27	0.0024	6.83	6.83	82.54	<0.0001	292.4	292.4	4.08	ns
X_{12}	1	0.005	0.005	0.12	ns	0.21	0.21	2.55	ns	28.13	28.13	0.39	ns
X_{13}	1	0.32	0.32	7.54	0.0206	1.36	1.36	16.46	0.0023	2415.1	2415.1	33.73	0.0002
X_{23}	1	0.02	0.02	0.47	ns	0.0012	0.0012	0.015	ns	6.13	6.13	0.086	ns
Residual	10	0.42	0.042	-	-	0.83	0.083	-	-	716.02	71.60	-	-
LoF	5	0.26	0.053	1.65	ns	0.50	0.10	1.52	ns	484.69	96.64	2.10	ns
Pure error	5	0.16	0.032	-	-	0.33	0.066	-	-	231.33	46.27	-	-
Core total	19	29.52	-	-	-	208.83	-	-	-	47191	-	-	-
		Zn (ppm)				Fe (ppm)				Ca (ppm)			
X_1	1	2549.4	2549.4	88.71	<0.0001	583.38	583.38	101.85	<0.0001	191.13	191.13	258.07	<0.0001
X_2	1	2229.1	2229.1	77.57	<0.0001	601.28	601.28	104.97	<0.0001	133.82	133.82	180.68	<0.0001
X_3	1	1638.0	1638.0	57.00	<0.0001	42.85	42.85	7.48	0.0210	7.86	7.86	10.61	0.0086
X_{11}	1	38.43	38.43	1.34	ns	27.54	27.54	4.81	ns	29.0	29.0	39.16	<0.0001
X_{22}	1	1034.9	1034.9	36.01	0.0001	12.74	12.74	2.22	ns	6.94	6.94	9.37	0.0120
X_{33}	1	1.1	1.1	0.038	ns	92.34	92.34	16.12	0.0025	59.81	59.81	80.76	<0.0001
X_{12}	1	346.5	346.5	12.68	0.0052	50.50	50.50	8.82	0.0141	7.03	7.03	9.49	0.0116
X_{13}	1	165.62	165.62	5.76	0.0373	2.10	2.10	0.37	ns	5.95	5.95	8.04	0.0177
X_{23}	1	623.04	623.04	21.68	0.0009	0.011	0.011	0.0019	ns	0.21	0.21	0.29	ns
Residual	10	287.38	28.74	-	-	57.28	5.73	-	-	7.41	0.74	-	-
LoF	5	173.94	34.79	1.53	ns	41.65	8.33	2.66	ns	5.51	1.10	2.90	ns
Pure error	5	113.45	22.69	-	-	15.63	3.13	-	-	1.90	0.38	-	-
Core total	19	8921.9	-	-	-	1453.4	-	-	-	436.89	-	-	-
		PA/Zn (-)											
X_1	1	0.065	0.065	59.61	<0.0001								
X_2	1	0.002	0.002	1.89	ns								
X_3	1	0.16	0.16	148.55	<0.0001								
X_{11}	1	0.14	0.14	127.51	<0.0001								
X_{22}	1	0.054	0.054	49.93	<0.0001								
X_{33}	1	0.001	0.001	1.12	ns								
X_{12}	1	0.002	0.002	1.85	ns								
X_{13}	1	0.030	0.030	27.17	0.0004								
X_{23}	1	0.0001	0.0001	0.12	ns								
Residual	10	0.011	0.0012	-	-								
LoF	5	0.009	0.0011	4.58	ns								
Pure error	5	0.002	0.0018	-	-								
Core total	19	0.46	-	-	-								

[a] X_1, X_2, and X_3 are SoTe – soaking temperature (°C), StTi – steaming time (min), and NF – nitrogen fertilization (kg ha^{-1}), respectively.
[b] DF, SS and MS are degree of freedom, sum of squares and mean squares, respectively; [c] ns – non-significant.

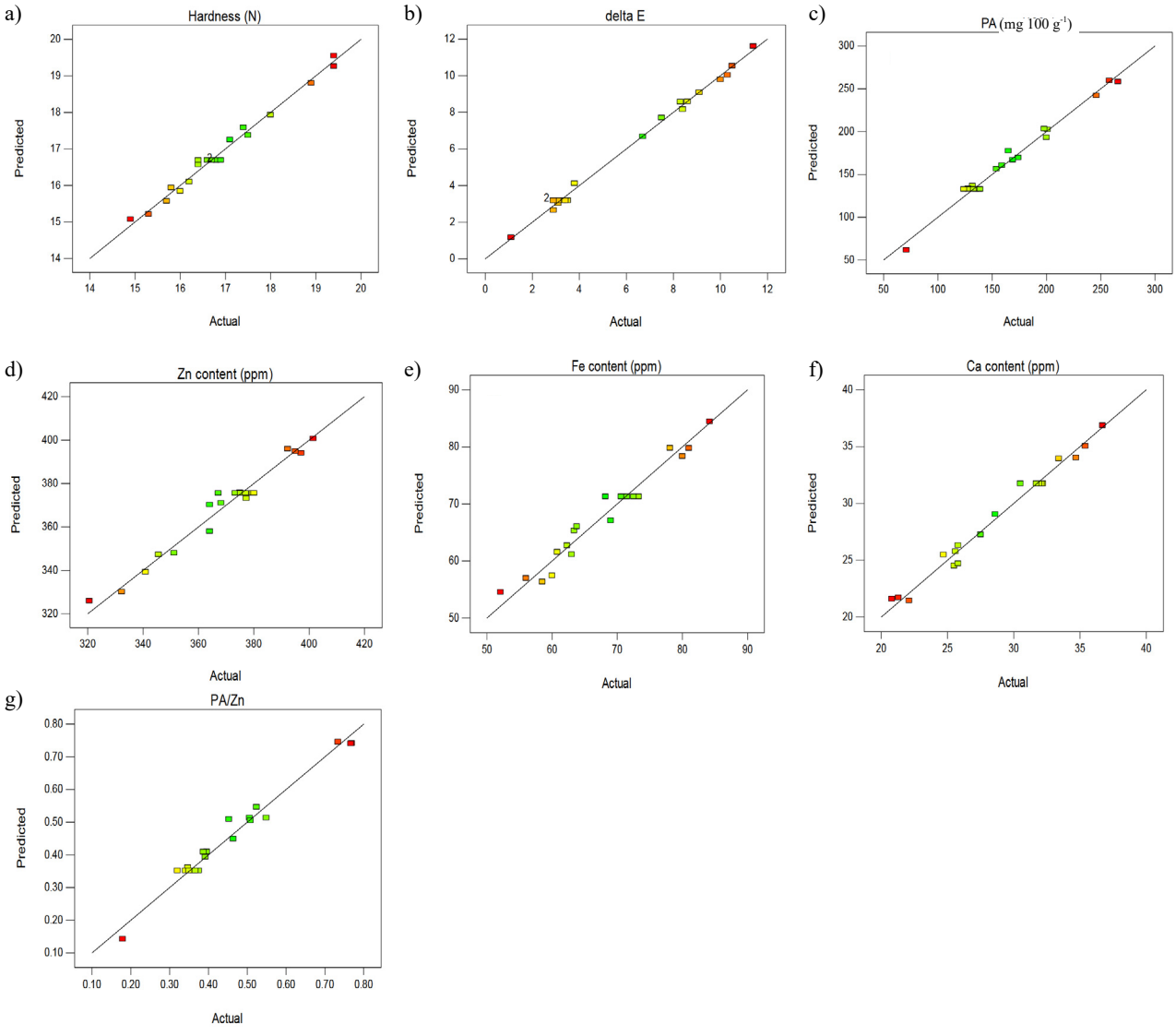

Fig. 2. Comparison between predicted and actual values of: a) hardness value, b) Δ*E* value, c) PA content, d) Zn content, e) Fe content, f) Ca content, and g) PA/Zn of parboiled BRGs.

The higher R^2 and R^2_{adj} values represented the high capability of quadratic equations in the given experimental range (Gharibzahedi *et al*., 2012). The CV values of 1.22-7.27% indicated high precision in the experiments (Table 3). The AP measures the signal-to-noise ratio, with a ratio greater than 4 considered desirable (Gharibzahedi *et al*., 2015). The AP values of 17.65-51.33 showed that the quadratic models were suitable for navigating the design space (Table 3). Figure 2 shows that the fitted models adequately covered the experimental range. The constructed regression models were in good agreement with the experimental results (Fig. 2).

3.3. Hardness value

Table 3 shows that the hardness value was significantly affected by the linear effects of all the independent variables. An increase in SoTe, StTi, and NF led to a significant increase in this factor ($p<0.0001$; $p<0.01$). The interaction effect of SoTe and NF ($p<0.05$) and the quadratic effect of NF ($p<0.01$) on the hardness value were also significant. The most significant ($p<0.05$) effect on the hardness value was the linear effect of NF followed by the main effect of SoTe and the quadratic effect of NF (Table 3). As shown in Fig. 3a, the variation of the hardness value of parboiled BRGs was a function of SoTe and NF. An increase in the levels of these independent variables resulted in higher hardness values. According to the individual optimization data, the targeted hardness value response (17.15 N) was observed when the parboiled BRGs were produced at 77.45°C SoTe, 10.64 min StTi, and 81.74 kg ha^{-1} NF.

Miah *et al.* (2002) earlier investigated the effect of rice soaking in hot water on the starch gelatinization and hardness of rice grains. The results showed that increasing the SoTe increased the starch gelatinization rate, grain hardening, and cooking time. Therefore, grains do not soften

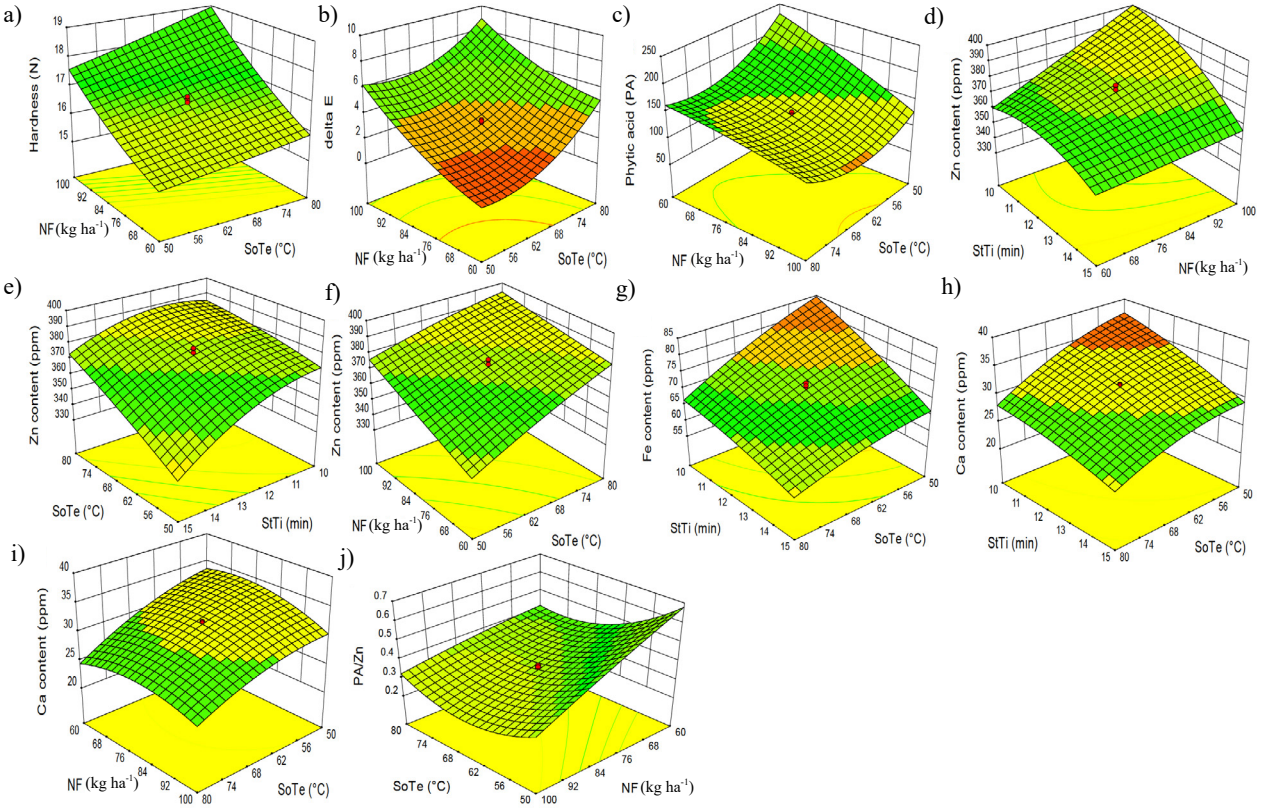

Fig. 3. 3D surface plots showing the significant interaction effects of independent parameters on the: a) variation of hardness value, b) Δ*E* value, and c) PA, d-f) Zn), g) Fe, and h, i) Ca contents, as well as j) PA/Zn.

and lose their shape during cooking. Besides, the parboiling at high temperatures/times increases compaction and the cohesion of starch particles in the center of granules increases molecular interaction between protein and starch to form a 3D network matrix and a harder texture against fracture (Sivakamasundari *et al*., 2020). However, soaking, compared to steaming, is more effective in increasing grain hardness by reducing chalky regions (Zhu *et al*., 2019). It is hypothesized that the deformation of proteins and starch during soaking at temperatures below the gelatinization point of starch (~75-80°C) plays a major role in reducing chalky spots and increasing grain hardness. The albumin and glutelin amounts present in rice grains decrease at 46 and 74°C, respectively, due to denaturation. Therefore, the high mobility of denatured proteins at SoTe greater than 80°C along with the opening of their spiral structure fills the empty spaces inside the endosperm due to chalky spots and increases the hardness degree. As glutelin is the predominant protein in rice, a further increase in hardness can be also observed when glutelin deforms at higher SoTe degrees (Adebiyi *et al*., 2009). Derycke *et al.* (2005) reported that more amylose chains in rice grains by intensifying the thermal process break down during soaking and have more mobility to penetrate deep inside of granules. The diffusion of these new intragranular chains can form a cohesive network with a much higher melting point, indicating greater grain strength (Derycke *et al.,* 2005). On the other hand, a reduction in the number of amylose units in starch granules can be observed at higher NF levels. Zohoun *et al.* (2018) pointed out that an increase of one unit in the amylose content can reduce hardness by 0.12 units. Furthermore, the surface hardening of rice grains at high NF levels may be due to the increased accumulation of protein in the surface layer. The water absorption and expansion in the thickness of rice grains can be inhibited in the presence of proteins in the outer layers, leading to an increased hardness value. Thus, the low content of amylose accompanied with high protein content in surface parts of rice grains cultivated in soils fertilized with high nitrogen amounts increased the hardness value.

Table 4 shows that increasing NF levels significantly increased the TP content and both instrumental and sensory hardness, while the TA content decreased. Additionally, the sensory and instrumental hardness values increased with the higher TP content and decreased with the higher TA content ($p<0.05$, Table 4). There was an adverse correlation ($r = - 0.7969$) between the content of TP and TA (Table 4). The correlation tests (Table 5) confirmed the positive influence of TP and the negative impact of TA on hardness values. Nitrogen is a key macronutrient involved in amino acid and protein biosynthesis. When applied to rice fields, nitrogen fertilizer enhances nitrogen uptake by

Table 4. Amounts of TA, TP, and instrumental and sensory values of hardness of parboiled BRGs[a]

NF level (kg ha^{-1})[b]	TP	TA	Hardness (N)	
	(%)		Instrumental	Sensory
46.5	8.95±0.42[b]	17.54±1.68[a]	14.90±0.23[c]	4.22±1.02[c]
60	9.46±0.25[b]	17.24±1.32[a]	15.42±0.48[c]	5.95±0.75[b]
80	10.36±0.13[a]	16.87±0.48[a]	17.63±0.55[b]	6.12±1.13[b]
100	10.42±0.28[a]	14.32±0.21[b]	18.73±0.41[a]	7.01±0.65[a]
113.6	10.73±0.17[a]	12.26±0.57[c]	19.40±0.11[a]	7.35±0.83[a]

[a]Treatments were performed at constant SoTe (65°C) and StTi (12.5 min), [b]mean values in the same column with different letters (a-c) are statistically significant ($p<0.05$).

Table 5. Correlation coefficients of TA, TP, and instrumental- and sensory-based hardness values of parboiled BRGs

Character	TP (%)	TA (%)	Hardness (N, Instrumental)	Hardness (N, Sensory)
TP (%)	1			
TA (%)	-0.7969	1		
Hardness (N, Instrumental)	0.9727	-0.8888	1	
Hardness (N, Sensory)	0.9234	-0.8291	0.9026	1

plants, increasing the pool of available nitrogen for incorporation into amino acids. This leads to elevated synthesis and accumulation of storage proteins in the rice endosperm, primarily glutelins and prolamins (Ma *et al.,* 2024; Yang *et al*., 2024). Consequently, the total protein content in rice grains rises with higher nitrogen levels. In contrast, amylose content often declines with increasing nitrogen fertilization. This is due to a shift in carbon allocation during grain filling. Under high nitrogen availability, rice plants prioritize protein synthesis, which competes with starch synthesis for carbon skeletons and energy. As a result, amylose biosynthesis *via* granule-bound starch synthase (GBSS) may be downregulated (Ma *et al.,* 2024). Furthermore, high nitrogen can alter the expression of starch-synthesizing enzymes, affecting the amylose-to-amylopectin ratio and leading to a relative decrease in amylose content. This reduction can influence the cooking and textural properties of rice, often making it softer and stickier.

3.4. Δ*E* color value

The Δ*E* color value was significantly influenced by the linear ($p<0.0001$, $p<0.001$) and quadratic ($p<0.0001$) effects of all the independent variables (Table 3). Furthermore, the interaction of SoTe and NF proved to be significant ($p<0.05$) among the interactions. The most significant effect on the Δ*E* value was shown to be the linear effect of NF followed by the quadratic effect of StTi and the linear effect of SoTe (Table 3). Figure 2b also illustrates that raising SoTe and NF in the range resulted in a higher Δ*E* value. Rice grains grown in soils fertilized with 64.46 kg ha^{-1} and parboiled under 53.52°C SoTe and 12.51 min StTi was predicted to result in the minimum Δ*E* color value (0.9833) based on the individual optimization findings.

More color changes at high NF levels can be attributed to the high accumulation of proteins in the granule depth. At higher levels of nitrogen, the grain lightness is reduced while its yellowness is increased (Kaur *et al*., 2016). Lamberts *et al.* (2006) explained that the soaking intensity increases the hydrolysis rate of starch and the concentration of reducing sugars through penetrating more moisture into granules. Accordingly, the presence of formed small sugars in the Maillard process increases color changes. They also emphasized that soaking rather than steaming accelerates more Maillard reactions by forming a higher number of simple sugars. The leakage of pigments from the rice husk was a function of different soaking temperatures and times, which had a direct effect on the ratio of water penetration and absorption in to the grain (Wiruch *et al*., 2019). The intensity of color changes by attaching the yellow and red pigments of the husk was increased by increasing the rate of water absorption at high SoTe. A similar result was reported by Islam *et al.* (2002b), who reported less intensity of color changes in steaming than soaking because thermal treatments may cause varying intensity of gelatinization in the surface and depth of starch granules. The starch gelatinization during the steaming step will be greater on the surface of rice grains. Greater retrogradation of gelatinized starch will form a hard surface texture. As this solid surface layer may act as a barrier against the migration of pigments during StTi, with further increasing the StTi it will not differ much in Δ*E*. Therefore, fewer color changes will be found during steaming compared to soaking (Islam *et al.*,

2002b). Shaiful Islam *et al.* (2009) showed that the external husk of rice during parboiling may become increasingly fissured, exposing simple sugars and amino acids to more reactions. Also, the pigments of the grain surface due to prolonged steaming have greater penetration capability into the deeper parts of the endosperm and intensify the color changes. Moreover, the color changes in rice grains are more intense in the first 10 min of steaming and then these changes continue at a lower rate between 10 and 30 min (Islam *et al.*, 2002a).

3.5. PA content

The results represented in Table 3 revealed that the PA content in parboiled BRGs was significantly ($p<0.0001$, $p<0.001$) influenced by the linear and quadratic terms between all the variables, except for the quadratic effect of the NF level, which was not significant. Among the interaction terms, only SoTe × NF was the strongest for the PA content (Table 3). The quadratic term of SoTe and the linear term of NF had the most significant effect on the PA content (Table 3). Figure 3c shows that an increase in the levels of SoTe and NF resulted in a significant reduction in the PA content in parboiled BRGs. The individual optimization results indicated that the optimum levels of SoTe, StTi, and NF for the minimum PA content were 65.06°C, 13.28 min, and 100 kg ha^{-1}, respectively.

The correlation analysis revealed a moderate negative correlation between the PA and TP content in parboiled BRGs ($r = -0.6508$). The reduction of PA content with increased protein levels in parboiled rice grains may be linked to higher NF levels. NF improves protein synthesis, and increased nitrogen availability could enhance protein accumulation at the expense of phytic acid. Elevated nitrogen may also promote enzymatic activity that breaks down PA, further reducing its content (Su *et al*., 2022). Decreasing the levels of anti-nutritional factors of rice such as PA can significantly guarantee the bioavailability of Zn and Fe because this chelator of divalent minerals limits their absorption. Ning *et al.* (2009) previously reported that an increasing NF level could reduce the PA content and an improvement in protein quality by increasing the ratio of glutelin to total protein. Zhang *et al.* (2010) suggested PA reduction by adding nitrogen fertilizer to the soil as concentrations of Fe and Zn in rice grains were significantly increased by increasing the NF level from 0 to 160 kg ha^{-1}. The PA reduction in parboiled rice can be attributed to its degradation or enzymatic hydrolysis by endogenous phytases activated during the soaking process at high SoTe temperatures and leaching into the soaking water (Taleon *et al*., 2020). In contrast, the high temperature of the water during the soaking phase does not inactivate phytase. Since phytase forms a molecular complex through interaction with other plant metabolites, it is less likely to be damaged by heat and remains intact after heating, effectively hydrolyzing PA (Liu *et al*., 2019). It seems that the use of parboiling at 65.06°C for 13.28 min seems to provide suitable conditions for maximum phytase activity present in rice grains to break down PA.

3.6. Mineral content

The linear effect of all independent variables on Zn ($p<0.0001$), Fe ($p<0.0001$, $p<0.05$), and Ca ($p<0.0001$, $p<0.01$) contents was highly significant (Table 3). Although the content of Ca was significantly affected by the quadratic term of all independent variables, the amounts of Zn and Fe were significantly changed by the quadratic effect of StTi and NF, respectively ($p = 0.0001$; $p<0.01$). The Zn content was affected by all cross terms of independent variables (SoTe × StTi, SoTe × NF, and StTi × NF). Fig. 3d-f illustrates that the Zn content increased with the increasing SoTe and NF levels but decreased with an increase in the StTi quantity. The interaction of parboiling parameters significantly affected the content of Fe, while the Ca amount was significantly affected by the interaction of SoTe with StTi and NF (Table 3). Figure 3g also shows that the parboiling process at high SoTe and StTi can significantly reduce the Fe content. Moreover, the increase in the amounts of NF and parboiling parameters led to a reduction in the level of Ca in parboiled BRGs (Fig. 3hi). From the individual optimization data, a combination of 50.57°C SoTe, 10 min StTi, and 96.62 kg ha^{-1} was predicted to achieve the maximum Zn (392.0 ppm), Fe (85.0 ppm), and Ca (34.77 ppm) levels in parboiled BRGs. On the other hand, the ratio of PA to Zn was significantly affected by the linear effects (SoTe and NF) and the quadratic (SoTe and StTi) effects of independent variables (Table 3). The interaction effect of SoTe and NF on the PA/Zn was significant ($p = 0.0004$). The linear effect of NF had the highest effect on the reduction of PA/Zn (Fig. 3j, Table 3).

The addition of nitrogen to the soil in rice fields could improve the content of Fe compared with Zn and Ca. The positive correlation between increased NF, higher protein content, and improved Fe content in parboiled BRGs ($r = 0.7371$) can be attributed to several factors. Nitrogen promotes protein synthesis, enhancing Fe-binding proteins like ferritin, which aid in Fe storage and mobilization. Besides, nitrogen potentiates photosynthesis, increasing energy availability for uptaking nutrients like Fe. It also improves soil conditions, making Fe more bioavailable, and stimulates root growth, leading to better absorption of Fe. Moreover, nitrogen interacts synergistically with micronutrients, further increasing Fe uptake and assimilation (Bhattacharya, 2021). Chandel *et al*. (2010) reported direct relationship between NF and Fe previously. This can be attributed to such factors as increased root growth, chemical changes in the rhizosphere, nitrification, pH reduction, and nitrogen-stimulated physiological changes affecting iron uptake (Islam *et al.*, 2002b; Chandel *et al*., 2010). The reduction of mineral elements such as Fe due to

Table 6. Optimizing the physico-mechanical characteristics of nanocomposite edible films based on plasticized WPI-JPS/SNC blends

Character	Goal	Overall optimization (Predicted data)	Experimental data (n = 5)[a]	Residue[b]
Hardness (N, Y_1)	Target	17.0	16.98±0.29	-0.02
ΔE (-, Y_2)	Minimize	4.71	4.69±0.09	-0.02
PA (mg 100 g^{-1}, Y_3)	Minimize	130.91	112.36±28.47	-18.55
Zn (ppm, Y_4)	Maximize	385.0	385.65±6.11	+0.65
Fe (ppm, Y_5)	Maximize	78.0	82.12±9.56	+4.12
Ca (ppm, Y_6)	Maximize	33.0	37.41±5.84	+4.41
PA/Zn (-, Y_7)	Minimize	0.340	0.291±0.057	-0.049

[a]Under the final optimal conditions: 59.29°C SoTe, 11.18 min StTi, and 90.89 kg ha^{-1} NF. [b]Residue: (Experimental-Predicted) data.

nitrogen deficiency can be also related to premature aging of leaves, as well as the reduction of chlorophyll and photosynthesis. These mechanisms lead to reduced micronutrient transfer to seeds, insufficient growth and development of rice roots in the soil, and thus reduced abi-lity to absorb elements from soil (Etienne *et al.,* 2018). The presence of high levels of nitrogen in soil stimulates Zn transportation from roots to grains by transporter proteins, such as the YSLs and ZIP family proteins, to increase the Zn uptake (Jaksomsak and Rerkasem, 2017). The cause for the leakage of minerals (*i.e.*, Fe, Zn, and Ca) during prolonged parboiling at high SoTe and StTi is the destruction of endosperm tissue. Starch gelatinization appears to be a key stage because the minerals accumulated in the aleurone layer are dissolved during this stage and can migrate to the shell layer during the steaming. Therefore, mineral movement depends on the steaming duration and the intensity of endosperm gelatinization. Besides, Albarracín *et al.* (2013) showed that the effect of soaking time and temperature on the reduction of minerals varies. They found that the Fe loss rate was higher than that of other minerals, so that Fe may even lose about 50% of its initial value in raw rice. However, the decrease in Zn was about 36%, which was consistent with the severity of mineral depletion in our research. Albarracín *et al.* (2013) also explained that, although harsh parboiling conditions reduce the mineral content in rice grains, the degradation of PA can increase the bioavailability of Fe, Zn, and Ca. Therefore, an optimization study was required to achieve the lowest PA/Zn ratio. The minimum PA/Zn in this study was predicted to be obtained at 65.7°C SoTe, 12.68 min StTi, and 100 kg ha^{-1} NF. This shows that soil fortification with high amounts of N fertilizer combined with medium parboiling conditions not only maintains the mineral content, particularly Zn, in BRGs but also provides the best conditions for attaining the maximum activity of phytase for PA hydrolysis.

3.7. Optimization and verification of the predictive models

The graphical representations of regression equations using response surface and contour plots were obtained using Design-Expert 8.0. The results of textural, color, and nutritional properties affected by the SoTe, StTi, and NF levels are presented in Table 6. The objective of this RSM-based modeling study was to determine the optimum fertilization and processing conditions leading to high-quality nutritious BRGs in terms of: (i) the target value for hardness, (ii) the highest Zn, Fe, and Ca contents, and (iii) the lowest PA, PA/Zn, and ΔE amounts. RSM-CCRD played a key role in identifying the optimum values of the independent variables. The optimization solution included a SoTe of 59.29°C, a StTi of 11.18 min, and an NF of 90.89 kg ha^{-1}. The suitability of second-order polynomial models for predicting the optimum response value was tested using the recommended optimum conditions. When optimum values of independent variables (59.29°C SoTe, 11.18 min StTi, and 90.89 kg ha^{-1} NF) were incorporated into the regression equations, a hardness value of 17.0 N, 385.0 ppm Zn, 78.0 ppm Fe, 33.0 ppm Ca, 130.91 mg 100 g^{-1} PA, PA/Zn of 0.34, and a ΔE value of 4.71 can be achieved (desirability = 0.778). The results showed that the corresponding experimental values for hardness, Zn, Fe, Ca, PA, PA/Zn, and ΔE of the desirable parboiled BRGs were 16.98 ± 0.29 N, 385.65 ± 6.11 ppm, 82.12 ± 9.56 ppm, 37.41 ± 5.84 ppm, 112.36 ± 28.47 mg 100 g^{-1}, 0.291 ± 0.057, and 4.69 ± 0.09, respectively (Table 6). There was only a small deviation ($p > 0.05$) between the experimental and predicted values for the response variables. Thus, the fitted quadratic models can be used to optimize the fertilization and parboiling parameters in the production of BRGs.

4. CONCLUSIONS

The simultaneous effect of the NF addition and the parboiling process to achieve high-quality BRGs with the lowest antinutritional PA component and the highest levels of Ca, Zn, and Fe micronutrients was optimized using the RSM-CCRD. Based on the model-based methodology used, second-order polynomial models could adequately predict the optimal points of this dynamic integrated strategy between agriculture and industry. The interactive effect of NF and SoTe significantly affected the hardness, ΔE, PA, Zn, PA/Zn, and Ca levels. The association between instrumental and sensory measures of BRG texture showed that

the consumers preferred BRGs with the optimum hardness value. Most of the studied quality and nutritional characteristics were significantly affected by the linear term of independent variables. NF application increases protein and decreases amylose content in rice grains, leading to higher instrumental hardness values and firmer sensory texture due to enhanced protein-starch interactions and reduced amylose-mediated softness. The numerical optimization defined the optimum conditions where the highest Zn, Ca, and Fe levels, the lowest PA, PA/Zn, and ΔE, as well as the optimum hardness were expected. In the optimum conditions (59.29°C SoTe, 11.18 min StTi, and 90.89 kg ha^{-1} NF), the corresponding predicted response values for Zn, Fe, Ca, PA, PA/Zn, and ΔE, and hardness were 385.65 ppm, 78.0 ppm, 33.0 ppm, 130.91 mg 100 g^{-1}, 0.34, 4.71, and 16.98 N, respectively. Lastly, the good agreement between the experimental and theoretical data also showed that the RSM-CCRD was a useful tool in optimization experiments. However, the results from this study are based on a single growing season, and while the model provided valuable insights, variability in soil and weather conditions across multiple years could influence the outcomes. Soil factors, such as nutrient content, pH, and texture, as well as climatic conditions (*e.g*., temperature, rainfall, and humidity), can affect the uptake of nitrogen and other nutrients, which in turn influences the quality and nutritional content in rice grains. Therefore, further investigations over multiple growing seasons (at least three years) are necessary to confirm the robustness and reliability of these findings across diverse environmental conditions. These multi-season studies would provide a more comprehensive understanding of the long-term effects of NF and parboiling conditions on rice grain quality.

Ethics Statement: Informed written consent from the sensory evaluation participants was obtained and all ethical guidelines were followed during the test. According to Iranian laws, ethical approval is not required for the sensory evaluation of common food products or the publication of this article.

Conflicts of Interest: The Authors do not declare any conflict of interest.

Data Availability Statement: The data presented in this study are available on request from the first author.

5. REFERENCES

Adebiyi, A.P., Adebiyi, A.O., Hasegawa, Y., Ogawa, T., Muramoto, K., 2009. Isolation and characterization of protein fractions from deoiled rice bran. Eur. Food Res. Technol. 228, 391-401. https://doi.org/10.1007/s00217-008-0945-4

Albarracín, M., González, R.J., Drago, S.R., 2013. Effect of soaking process on nutrient bio-accessibility and phytic acid content of brown rice cultivar. Food Sci. Technol. 53, 76-80. https://doi.org/10.1016/j.lwt.2013.01.029

Bhattacharya, A., 2021. Mineral nutrition of plants under soil water deficit condition: A Review. In: Soil water deficit and physiological issues in plants, Springer, Singapore, pp. 287-391. https://doi.org/10.1007/978-981-33-6276-5_4

Chandel, G., Banerjee, S., See, S., Meena, R., Sharma, D.J., Verulkar, S.B., 2010. Effects of different nitrogen fertilizer levels and native soil properties on rice grain Fe, Zn and protein contents. Rice Sci. 17, 213-227. https://doi.org/10.1016/S1672-6308(09)60020-2

Chavan, P., Sharma, S.R., Mittal, T.C., Mahajan, G., Gupta, S.K., 2018. Effect of parboiling technique on Physico-Chemical and nutritional characteristics of basmati rice. J. Agric. Res. 55, 490-499. https://doi.org/10.5958/2395-146X.2018.00089.3

Derycke, C., Vandeputte, G.E., Vermeylen, R., De Man, W., Goderis, B., Koch, M.H.J., *et al*., 2005. Starch gelatinization and amylose-lipid interactions during rice parboiling investigated by temperature resolved wide angle X-ray scattering and differential scanning calorimetry. J. Cereal Sci. 42, 334-343. https://doi.org/10.1016/j.jcs.2005.05.002

Etienne, P., Diquelou, S., Prudent, M., Salon, C., Maillard, A., Ourry, A., 2018. Macro and micronutrient storage in plants and their remobilization when facing scarcity: the case of drought. Agriculture 8, 14. https://doi.org/10.3390/agriculture8010014

Gharibzahedi, S.M.T., 2018. Favorite and traditional rice flour–based puddings, breads, and pastries in the north of Iran: A review. J. Ethn. Foods 5, 105-113. https://doi.org/10.1016/j.jef.2018.03.001

Gharibzahedi, S.M.T., Razavi, S.H., Mousavi, M., 2012. Developing an emulsion model system containing canthaxanthin biosynthesized by *Dietzia natronolimnaea* HS-1. Int. J. Biol. Macromol. 51, 618-626. https://doi.org/10.1016/j.ijbiomac.2012.06.030

Gharibzahedi, S.M.T., Rostami, H., Yousefi, S., 2015. Formulation design and physicochemical stability characterization of nanoemulsions of nettle (*Urtica dioica*) essential oil using a model-based methodology. J. Food Process. Preserv. 39, 2947-2958. https://doi.org/10.1111/jfpp.12546

Gharibzahedi, S.M.T., Roohinejad, S., George, S., Barba, F.J., Greiner, R., Barbosa-Cánovas, G.V., *et al*., 2018. Innovative food processing technologies on the transglutaminase functionality in protein-based food products: Trends, opportunities and drawbacks. Trends Food Sci. Technol. 75, 194-205. https://doi.org/10.1016/j.tifs.2018.03.014

Glauber, J.W., Mamun, A., 2025. Global rice market: Current outlook and future prospects, IFPRI Discussion Paper 2310, Washington, DC: Int. Food Policy Res. Institute https://hdl.handle.net/10568/168523

Islam, M.R., Shimizu, N., Kimura, T., 2002a. Effect of processing conditions on thermal properties of parboiled rice. Food Sci. Technol. Res. 8, 131-136. https://doi.org/10.3136/fstr.8.131

Islam, M.R., Roy, P., Shimizu, N., Kimura, T., 2002b. Kimura, Effect of processing conditions on physical properties of parboiled rice. Food Sci. Technol. Res. 8, 106-112. https://doi.org/10.3136/fstr.8.106

Jaksomsak, P., Rerkasem, B., 2017. Responses of grain zinc and nitrogen concentration to nitrogen fertilizer application in rice varieties with high-yielding low-grain zinc and low-yielding high grain zinc concentration. Plant Soil 411, 101-109. https://doi.org/10.1007/s11104-016-3056-1

Kaur, A., Ghumman, A., Singh, N., Kaur, S., Virdi, A.S., Riar, G.S., *et al*., 2016. Effect of different doses of nitrogen on protein profiling, pasting and quality attributes of rice from different cultivars. J. Food Sci. Technol. 53, 2452-2462. https://doi.org/10.1007/s13197-016-2230-z

Kaur, M., Asthir, B., Mahajan, G., 2017. Variation in antioxidants, bioactive compounds and antioxidant capacity in germinated and ungerminated grains of ten rice cultivars. Rice Sci. 24, 349-359. https://doi.org/10.1016/j.rsci.2017.08.002

Kumar, A., Lal, M.K., Kar, S.S., Nayak, L., Ngangkham, U., Samantaray, S., *et al*., 2017. Bioavailability of iron and zinc as affected by phytic acid content in rice grain. J. Food Biochem. 41: e12413. https://doi.org/10.1111/jfbc.12413

Lamberts, L., Rombouts, I., Brijs, K., Gebruers, K., Delcour, J.A., 2006. Impact of browning reactions and bran pigments on color of parboiled rice. J. Agric. Food Chem. 54: 9924-99929. https://doi.org/10.1021/jf062140j

Liu, K., Zheng, J., Wang, X., Chen, F., 2019. Effects of household cooking processes on mineral, vitamin B, and phytic acid contents and mineral bioaccessibility in rice. Food Chem. 280, 59-64. https://doi.org/10.1016/j.foodchem.2018.12.053

Ma, Z., Zhu, Z., Song, W., Luo, D., Cheng, H., Wang, X., Lyu, W., 2024. Effects of nitrogen fertilizer on the endosperm composition and eating quality of rice varieties with different protein components. Agronomy 14, 469. https://doi.org/10.3390/agronomy14030469

Miah, M.K., Haque, A., Douglass, M.P., Clarke, B., 2002. Parboiling of rice. Part II: Effect of hot soaking time on the degree of starch gelatinization. Int. J. Food Sci. Technol. 37, 539-545. https://doi.org/10.1046/j.1365-2621.2002.00611.x

Nasrollah Zadeh, A., Ghorbani-Hasansaraei, A., Amiri, E., Habibi, F., 2020. The improved chemical, mechanical, rheological, and pasting characteristics of protein-rich brown rice by parboiling process integrated with nitrogen fertilization. Bull. Univ. Agric. Sci. Vet. Med. Cluj-Napoca, Food Sci. Technol. 77, 45-56. https://doi.org/10.15835/buasvmcn-fst:2020.0034

Ning, H., Liu, Z., Wang, Q., Lin, Z., Chen, S., Li, G., *et al*., 2009. Effect of nitrogen fertilizer application on grain phytic acid and protein concentrations in japonica rice and its variations with genotypes. J. Cereal Sci. 50, 49-55. https://doi.org/10.1016/j.jcs.2009.02.005

Özkaya, B., Turksoy, S., Özkaya, H., Duman, B., 2017. Dephytinization of wheat and rice brans by hydrothermal autoclaving process and the evaluation of consequences for dietary fiber content, antioxidant activity and phenolics. Innov. Food Sci. Emerg. Technol. 39, 209-215. https://doi.org/10.1016/j.ifset.2016.11.012

Paiva, F.F., Vanier, N.L., Berrios, J.D.J., Pinto, V.Z., Wood, D., Williams, T., *et al*., 2016. Polishing and parboiling effect on the nutritional and technological properties of pigmented rice. Food Chem. 191, 105-112. https://doi.org/10.1016/j.foodchem.2015.02.047

Park, J., Gim, S.Y. , Jeon, J.Y., Kim, M.J., Choi, H.K., Lee, J., 2019. Chemical profiles and antioxidant properties of roasted rice hull extracts in bulk oil and oil-in-water emulsion. Food Chem. 272, 242-250. https://doi.org/10.1016/j.foodchem.2018.08.054

Patindol, J., Fragallo, L., Wang, Y.J., Durand-morat, A., 2017. Impact of feedstock, parboiling condition, and nutrient concentration on simultaneous fortification of two US long-grain rice cultivars with iron and zinc. Cereal Chem. 94, 984-990. https://doi.org/10.1094/CCHEM-05-17-0115-R

Rostami, H., Gharibzahedi, S.M.T., 2017. Cellulase-assisted extraction of polysaccharides from Malva sylvestris: Process optimization and potential functionalities. Int. J. Biol. Macromol. 101, 196-206. https://doi.org/10.1016/j.ijbiomac.2017.03.078

Shaiful Islam, M.D., Hasanuzzaman, M., Rokonuzzaman, M., Nahar, K., 2009. Effect of split application of nitrogen fertilizer on morph physiological parameters of rice genotypes. Int. J. Plant Prod. 3, 51-62. https://dx.doi.org/10.22069/ijpp.2012.631

Shao, Y., Hu, Z., Yu, Y., Mou, R., Zhu, Z., Beta, T., 2018. Phenolic acids, anthocyanins, proanthocyanidins, antioxidant activity, minerals and their correlations in non-pigmented, red, and black rice. Food Chem. 239, 733-741. https://doi.org/10.1016/j.foodchem.2017.07.009

Sivakamasundari, S.K., Moses, J.A., Anandharamakrishnan, C., 2020. Effect of parboiling methods on the physicochemical characteristics and glycemic index of rice varieties. J. Food Meas. Charact. 14, 3122-3137. https://doi.org/10.1007/s11694-020-00551-9

Su, D., Muneer, M.A., Chen, X., Rasmussen, S.K., Wu, L., Cai, Y., Cheng, F., 2022. Response of phytic acid to nitrogen application and its relation to protein content in rice grain. Agronomy 12, 1234. https://doi.org/10.3390/agronomy12051234

Taghinezhad, E., Khoshtaghaza, M.H., Minaei, S., Suzuki, T., Brenner, T., 2016. Relationship between degree of starch gelatinization and quality attributes of parboiled rice during steaming. Rice Sci. 23, 339-344. https://doi.org/10.1016/j.rsci.2016.06.007

Taheri-Garavand, A., Nassiri, A., Gharibzahedi, S.M.T., 2012. Physical and mechanical properties of hemp seed. Int. Agrophys. 26, 211-215. https://doi.org/10.2478/v10247-012-0031-9

Taleon, V., Gallego, S., Orozco, J.C., Grenier, C., 2020. Retention of Zn, Fe and phytic acid in parboiled biofortified and non-biofortified rice. Food Chem: X, 8, 100105. https://doi.org/10.1016/j.fochx.2020.100105

Tayefe, M., Shahidi, S.A., Milani, J.M., Sadeghi, S.M., 2020. Development, optimization, and critical quality characteristics of new wheat-flour dough formulations fortified with hydrothermally-treated rice bran. J. Food Meas. Charact. 14, 2878-2888. https://doi.org/10.1007/s11694-020-00532-y

Tian, J., Cai, Y., Qin, W., Matsushita, Y., Ye, X., Ogawa, Y., 2018. Parboiling reduced the crystallinity and in vitro digestibility of non-waxy short grain rice. Food Chem. 257, 23-28. https://doi.org/10.1016/j.foodchem.2018.03.005

Wei, H.Y., Zhang, H.C., Dai, Q.G., Qun, M.A., Jie, L.I., Zhang, Q., *et al*., 2010. Response of iron content in milled rice to nitrogen levels and its genotypic differences. Rice Sci. 17(3), 228-234. https://doi.org/10.1016/S1672-6308(09)60021-4

Wiruch, P., Srisuwan, N., Yongyut, C., 2019. Textural properties, resistant starch, and *in vitro* starch digestibility as affected by parboiling of brown glutinous rice in a retort pouch. Curr. Res. Nutr. Food Sci. 7, 555-567. https://dx.doi.org/10.12944/CRNFSJ.7.2.24

Xia, Q., Green, B.D., Zhu, Z., Li, Y., Gharibzahedi, S.M.T., Roohinejad, S., Barba, F.J., 2019. Innovative processing

techniques for altering the physicochemical properties of wholegrain brown rice (*Oryza sativa* L.) – opportunities for enhancing food quality and health attributes. Crit. Rev. Food Sci. Nutr. 59, 3349-3370. https://doi.org/10.1080/10408398.2018.1491829

Yang, G., Chen, H., Zhang, G., Yang, G., Wang, X., Hu, Y., 2024. Effect of nitrogen fertilizers on the starch and protein contents, and physicochemical characteristics of rice noodles. J. Food Compos. Anal. 135, 106565. https://doi.org/10.1016/j.jfca.2024.106565

Yu, X., Yang, T., Qi, Q., Du, Y., Shi, J., Liu, X., 2021. Comparison of the contents of phenolic compounds including flavonoids and antioxidant activity of rice (*Oryza sativa*) and Chinese wild rice (*Zizania latifolia*). Food Chem. 344, 128600. https://doi.org/10.1016/j.foodchem.2020.128600

Zhu, L., Cheng, L., Zhang, H., Wang, L., Qian, H., Qi, X., Wu, G., 2019. Research on migration path and structuring role of water in rice grain during soaking. Food Hydrocolloid. 92, 41-50. https://doi.org/10.1016/j.foodhyd.2019.01.051

Zohoun, E.V., Tang, E.N., Soumanou, M.M., Manful, J., Akissoe, N.H., Bigoga J., *et al.*, 2018. Physicochemical and nutritional properties of rice as affected by parboiling steaming time at atmospheric pressure and variety. Food Sci. Nutr. 6, 638-652. https://doi.org/10.1002/fsn3.600